Fusion, fission, and scrambling of the bilaterian genome in Bryozoa

Thomas D. Lewin[a], Isabel Jiah-Yih Liao[a], Mu-En Chen[a], John D. D. Bishop[b], Peter W. H. Holland[c], and Yi-Jyun Luo[a,*]

Author affiliations:
[a]Biodiversity Research Center, Academia Sinica, Taipei, Taiwan
[b]Marine Biological Association, Plymouth, UK
[c]Department of Biology, University of Oxford, Oxford, UK
*To whom correspondence may be addressed.

Email: yjluo@gate.sinica.edu.tw

Abstract

Genes are commonly found together on the same chromosome over vast evolutionary distances. This extensive physical gene linkage, known as macrosynteny, can be seen between bilaterian phyla as divergent as Chordata, Echinodermata, Mollusca, and Nemertea and likely reflects the importance of genome organization to gene regulatory landscapes. Here, we report a very different pattern of genome evolution in Bryozoa, an understudied yet ecologically important phylum of colonial invertebrates. Using comparative genomics, we reconstruct the chromosomal evolutionary history of five bryozoans. We infer the ancestral bryozoan genome organization and identify multiple ancient chromosome fusions followed by gene mixing, leading to the near-complete loss of bilaterian linkage groups. A second wave of rearrangements, including chromosome fission, occurred independently in two bryozoan classes, further shuffling bryozoan genomes. We also discover nine chromosomal fusion events shared between bryozoans and brachiopods, supporting the traditional yet highly debated Lophophorata hypothesis. Finally, we show that chromosome fusion and fission processes led to the separation of bryozoan Hox clusters. These findings demonstrate how the canonical bilaterian genome structure has been lost across an entire phylum, suggest a modification to gene regulatory landscapes, and provide a powerful source of phylogenetic information.

Introduction

With advances in genome sequencing and assembly in recent years, it has become possible to compare the organization of entire chromosomes across the diversity of the animal kingdom. The emerging picture is one of a common set of metazoan genes, superimposed with extensive gene duplication, gene loss, and gene novelty in each lineage, plus a surprising degree of large-scale organizational similarity. Many genes have remained on the same chromosome for hundreds of millions of years and remain together in diverse and highly divergent lineages (1–6). This phenomenon, referred to as macrosynteny, is most likely related to the importance of genome organization for gene regulation and expression.

The persistence of gene linkages enables the identification of orthologous chromosomes between distantly related phyla. Furthermore, it permits the reconstruction of ancestral linkage groups (ALGs)—hypothesized sets of genes located on the same chromosome or chromosome arm in ancestral species (4, 7). ALGs specific to certain lineages have been identified in several animal groups, including vertebrates (8, 9) and Lepidoptera (butterflies and moths) (10). Most strikingly, the discovery of 24 ALGs shared between spiralians and deuterostomes (4, 11) reveals the genome organization of the most recent bilaterian common ancestor. Species from phyla as divergent as chordates, echinoderms, molluscs, and annelids have largely retained these highly-conserved bilaterian blocks of genes (4, 6, 11–13), suggesting substantial functional constraints. There are lineages within phyla that have experienced genomic shuffling, such as planarians (14) and tunicates (15), but conservation of the ALGs seems the norm at the phylum level. Despite this conservation, fluctuation in chromosome number is a relatively frequent evolutionary process (16–19). These changes can result from whole genome duplication, but in animals, most are attributed to inter-chromosomal rearrangements, including translocations and fusions (20–23). Following chromosome fusion, genes from different ALGs may either be maintained in separate chromosome sections or be shuffled and interspersed along the chromosome in a process known as ‘fusion-with-mixing’ (4). Conversely, chromosomes can undergo fission, splitting into separate parts, but the division of ALGs through this process is considered rare (4, 10).

The interplay between gene sets' stability and the dynamic nature of inter-chromosomal rearrangements shapes the genomic landscape. These rearrangements, while disrupting gene function and expression (24) and altering recombination rates (25), also play a critical role in driving adaptation (26–28) and contributing to macroevolutionary processes like speciation (29–32). This dynamic quality of chromosomal changes has also been exploited in phylogenetic studies, where macrosynteny can be a powerful tool (33). Fusion-with-mixing events could prove particularly powerful phylogenetic markers as they are considered to be irreversible rare genomic changes. Once genes from different ALGs become intermixed on a chromosome, they cannot revert to their original, separate states (4). In light of this, macrosynteny was recently used to investigate deeply branching metazoan lineages (5) and early teleost evolution (34).

Even in the age of phylogenomics, when the amino acid sequences of thousands of deduced proteins are aligned and analyzed, there remains a small group of ‘Problematica’: taxa for which a robust phylogenetic placement remains tantalizingly out of reach (35, 36). Many of these taxa are rare or have few species. Yet one phylum—the Bryozoa—stands out among Problematica as highly abundant, species-rich, and ecologically important, increasingly as alien invasive species (37–40). Bryozoans are benthic, suspension-feeding, aquatic invertebrates that are important ecosystem engineers. They form colonies of individual zooids with generally calcified skeletons (41), and each zooid can be morphologically differentiated for specialized roles in feeding, brooding, or defense. Despite their unique

biological traits, bryozoans, especially their genomes, remain relatively understudied. Several chromosome-scale assemblies have recently been made available (42–45), but these are without comparative analysis, and beyond an accepted placement within Spiralia, the phylum's phylogenetic position remains unresolved (35, 36, 40, 46) (*SI Appendix*, Fig. S1).

In this study, we investigate chromosome evolution in the phylum Bryozoa. We first generate gene models for five chromosome-scale bryozoan genomes. Using macrosynteny analysis, we find massive chromosome rearrangements in the evolutionary history of bryozoans that have dispersed bilaterian ALGs around their genomes. By reconstructing the bryozoan ancestral state, we show that chromosome fission events have fragmented ALGs, challenging the general idea that ALGs are sometimes combined but not broken up (4). We also compare the macrosynteny of bryozoans to that of brachiopods, demonstrating that the phyla share nine ALG fusion events. This finding supports the Lophophorata hypothesis for bryozoans' phylogenetic position, placing them with brachiopods and phoronids. Our data reveal that selective constraints that have maintained genes in bilaterian ALGs over at least 540 million years of evolution (47) have been released in the bryozoan phylum.

Results

Chromosome-scale genomes of five bryozoans.

To reconstruct the evolutionary history of chromosomes at the phylum level, we accessed chromosome-scale assemblies for four marine bryozoans from the Darwin Tree of Life project which has made genomic data publicly available for the community to analyze (48). These species are *Bugulina stolonifera* (BST), *Cryptosula pallasiana* (CPA), *Membranipora membranacea* (MME), and *Watersipora subatra* (WSU), all in the class Gymnolaemata, which accounts for approximately 89% of described bryozoan species (49) (Fig. 1*A*). We also used a chromosome-scale assembly for the freshwater bryozoan *Cristatella mucedo* (CMU) from the DNA Zoo project (42), a member of thebryozoan class, Phylactolaemata (50). Since accurate phylogenetic relationships are key to inferring chromosome rearrangement events, we built a maximum likelihood phylogenetic tree of the five bryozoan species using gene models obtained from the chromosome-scale genomes (Fig. 1*B*); this tree is consistent with recent phylogenetic analyses using mitochondrial and ribosomal data (51). We performed comprehensive gene prediction using the BRAKER3 pipeline, utilizing transcriptomic data as supporting evidence (Fig. 1*C* and *SI Appendix*, Tables S1–S7). Benchmarking Using Single-Copy Orthologs (BUSCO) (52) reveals a high degree of completeness in gene predictions while also indicating gene losses in bryozoans, as evidenced by completeness scores of 82.7% to 88.6% from the Metazoa database (odb10) (*SI Appendix*, Table S1); principal component analysis of orthologous gene counts finds bryozoans to have a gene set broadly similar to that of other Lophotrochozoa (Fig. 1*D*, *E* and *SI Appendix*, Table S8).

Massive chromosome rearrangements within Bryozoa.

Using Orthofinder (53), we identified 4,242 single-copy orthologs shared between the five bryozoan species. We mapped the position of these orthologs within each genome to construct synteny maps, displayed as ribbon plots and Oxford dot plots (*SI Appendix*, Fig. S2). Throughout our analysis of chromosome rearrangements, we applied the algebraic symbol conventions established by Simakov et al., wherever applicable (4). Specifically, we use triple bar for one-to-one relationships, also known as syntenic equivalences (≡); tensor for fusion with mixing (⊗); dot product for end-to-end fusion (●); down arrow for centric insertion (↘); and

addition for fission (+) (Fig. 1*F*). However, although these methods are effective for relatively conserved taxa, we found the highly derived nature of bryozoan genomes resulted in many contemporary chromosomes not fitting clearly into these predefined categories. Furthermore, the notation may become excessively complex and confusing when addressing chromosomes that have undergone numerous ALG fusions and have intricate evolutionary histories. Consequently, we also utilize narrative descriptions, especially for highly derived chromosomes.

We found that chromosome numbers show high conservation between the four species of the same class Gymnolaemata. For example, *B. stolonifera*, *M. membranacea,* and *W. subatra* all possess 11 chromosomes (haploid chromosome number n = 11). Based on orthologous genes, we identified orthologous chromosomes and assigned 11 Gymnolaemata ALGs, labeled ALGs *a* to *k* (Fig. 2*A*). Our findings indicate complete syntenic equivalence among these three species, indicating there have been no events of chromosome fusion or fission. The other Gymnolaemata species, *Cry. pallasiana*, has undergone one fission event to diverge from this state, with Gymnolaemata ALG *a* (*M. membranacea* chr1 ≡ *B. stolonifera* chr1 ≡ *W. subatra* chr1) splitting to form two smaller chromosomes (*Cry. pallasiana* chr10 and chr12) (Fig. 2*A*). This aside, chromosome structure is highly conserved between these species. In contrast, a striking lack of conservation is observed when the Phylactolaemata bryozoan *Cri. mucedo* is compared. None of the 11 Gymnolaemata ALGs are conserved, and most are completely dispersed and shuffled across the entire *Cri. mucedo* genome (Fig. 2*A*). For instance, we identified four Gymnolaemata ALGs on seven of eight *Cri. mucedo* chromosomes (Gymnolaemata ALGs *a*, *b*, *c*, and *g*) (*SI Appendix*, Fig. S3). This represents an almost complete loss of chromosome relationships between the two groups.

In analyzing deeply branching animals, particularly across phyla, macrosynteny studies often overlook the precise gene order, known as microsynteny (54, 55). This is due to intra-chromosomal rearrangements like inversions, which alter chromosome gene order over long evolutionary periods. Such chromosomal changes lead to weak microsyntenic signals, making them difficult to trace between distantly related species. However, there is a relatively recent divergence of *W. subatra* and *Cry. pallasiana*, estimated at 60–90 million years ago (51), allows for sufficient conservation of microsynteny to investigate intra-chromosomal rearrangements. By generating Oxford dot plots for whole genomes (Fig. 2*B*) and individual chromosomes (Fig. 2*C*), we identified six clear cases of large intra-chromosomal inversions between these two species (e.g., *W. subatra* chr1 vs. *Cry. pallasiana* chr12). We noticed many inversions with a complete lack of intermixing across chromosomes, suggesting that these inversions involved entire chromosome arms (e.g., *W. subatra* chr8 vs. *Cry. pallasiana* chr3) (Fig. 2*C* and *D*). We developed a microsynteny mixing score (see Materials and Methods) to quantify the extent of intra-chromosomal gene shuffling. We found that between the closely related species *W. subatra* and *Cry. pallasiana*, mixing score varies greatly between chromosomes, suggesting genes are not shuffled equally on different chromosomes. In addition, the mixing score increases linearly with the estimated divergence time in our dataset (Fig. 2*E* and *SI Appendix*, Tables S9 and S10), though this score would become saturated if more divergent species were compared.

Near-complete disruption of bilaterian ancestral linkage groups in Bryozoa.

We next investigated how bryozoan chromosomes relate to the conserved bilaterian genome organization. Using only the bryozoan data, it remains uncertain whether the Gymnolaemata,

Phylactolaemata, or neither maintains the ancestral state for the phylum. To resolve this, we compared the macrosynteny of bryozoans with three bilaterians with conserved genome organization: the nemertean *Lineus longissimus* (56), the mollusc *Pecten maximus* (57), and the amphioxus *Branchiostoma floridae* (9). Both *L. longissimus* and *P. maximus* belong to Lophotrochozoa, the same major protostome clade as bryozoans, while the deuterostome *B. floridae* serves as an outgroup. We generated a dataset of 995 single-copy orthologs and identified the association of each ortholog with one of the 24 bilaterian ALGs described by Simakov et al. (4) (Dataset S1). Synteny maps show that, despite their divergence at the base of the Bilateria, the genome organizations of *B. floridae*, *P. maximus*, and *L. longissimus* exhibit high levels of similarity, having largely preserved the ancestral bilaterian genome architecture (Fig. 3, *SI Appendix*, Fig. S4, Table S11). Our analysis revealed that *P. maximus* and *L. longissimus* share four fusion events that have also been recorded in annelids and brachiopods (J2⊗L, O1⊗R, O2⊗K, and H⊗Q) (4, 13), suggesting that they are ancestral to Lophotrochozoans. In addition, we detected many lineage-specific fusion events. Specifically, we identified fusions on chr1 (A1⊗A2), chr2 (C1⊗J2), chr3 (C2●Q), and chr4 (O1●I) in *B. floridae*; a fusion on chr2 (B2⊗M) in *P. maximus*; and a fusion on chr2 (C1⊗G) in *L. longissimus*. These changes are minor, considering the divergence times among these species.

Remarkably, numerous ALGs have been extensively mixed in the bryozoan lineage, despite having been conserved among both lophotrochozoans and deuterostomes since the emergence of the bilaterian last common ancestor (Fig. 3 and *SI Appendix*, Table S12). We discovered that 18 out of the 24 bilaterian ALGs (75%) had been combined and mixed across four Gymnolaemata orthologous chromosomes, indicating that Gymnolaemata bryozoans underwent substantial irreversible fusion-with-mixing events followed by fragmentation of a single, ancestrally fused chromosome into four distinct ones. We also detect other bryozoan-specific fusions: ALGs A1 and C2 initially fused (A1⊗C2) and then divided into two chromosomes (e.g., *M. membranacea* chr6 and chr8); ALG P joined with the lophotrochozoan fusion K⊗O2 (P⊗K⊗O2) and later separated into two chromosomes (e.g., *M. membranacea* chr9 and chr10); ALGs F and N fused (F⊗N) and subsequently split into two chromosomes (e.g., *M. membranacea* chr5 and chr11). Conversely, one chromosome contains only ALG M genes (e.g., *M. membranacea* chr7), although various genes from ALG M were translocated to other chromosomes. This distinct chromosomal arrangement is consistent across *M. membranacea*, *B. stolonifera*, *W. subatra*, and *Cry. pallasiana*, except for the unique fission event in *Cry. pallasiana* described above.

We found that the *Cri. mucedo* genome arrangement, while very different from other bryozoans, similarly does not preserve the bilaterian ALGs. Massive rearrangements have independently taken place within the lineage leading to *Cri. mucedo*, resulting in the dispersion of bilaterian ALGs throughout its genome (Fig. 3). Overall, the genome organization in the two classes of bryozoans studied here is distinct, and both of these organizations are highly divergent from the bilaterian ancestral state.

The ancestral bryozoan genome was highly rearranged.

Since the Gymnolaemata and Phylactolaemata bryozoans have such distinct genome arrangements, we sought to uncover the genomic structure of the bryozoan ancestor. Did it maintain the general bilaterian organization or had rearrangements already occurred? We leveraged the conserved gene linkages found in modern genomes to reconstruct the bryozoan ancestral state. This analysis revealed the likely presence of six ALGs, suggesting an

ancestral karyotype of six chromosomes (designated here as α, β, γ, δ, ε, and ζ) (Fig. 4*A, B*). Notably, bryozoan ALGs α and β comprise 10 and eight bilaterian ALGs, respectively, indicating numerous events of sequential fusion-with-mixing (Fig 4*C* and *SI Appendix*, Fig. S5 and Table S13). Thus, extensive chromosomal rearrangements had fused and shuffled bilaterian ALGs extensively, even before the extant clades of bryozoans diverged.

Based on this bryozoan ancestral state, we reconstructed the events leading to the observed genome structures in contemporary species (Fig. 4*D*). In the Gymnolaemata, the chromosomes containing ALGs α and β underwent fusion-with-mixing (α⊗β) to create one enormous chromosome containing 18 bilaterian ALGs. This chromosome then underwent sequential fission events to form four daughter chromosomes containing these 18 bilaterian ALGs (e.g., *M. membranacea* chr1 to chr4). Meanwhile, bryozoan ALGs δ, ε, and ζ underwent a single fission event to form two separate chromosomes. ALG γ was maintained alone on one chromosome (chr7), but genes from this ALG also dispersed to all other chromosomes (Fig. 4*D*). The *Cri. mucedo* genome exhibits a structure more derived from the bryozoan ancestral state, characterized by numerous fission and fusion events with limited mixing, resulting in chromosomes consisting of distinct segments derived from different bryozoan ALGs (Fig. 4*E*). Overall, the bryozoan common ancestor had a highly derived genome, and lineage-specific fusion and fission events have further modified the genomes of both Gymnolaemata and Phylactolaemata bryozoans.

Shared derived chromosomal rearrangements between bryozoans and brachiopods.

Recent studies have proposed the application of macrosynteny analysis in phylogeny, arguing that the infrequency and irreversibility of fusion-with-mixing allow these events to serve as phylogenetic markers. In light of the contentious debate surrounding the phylogenetic position of bryozoans, we sought to determine if macrosynteny could offer insights in this regard. Two contrasting hypotheses exist: (a) the Lophophorata hypothesis, which proposes a close relationship to phoronids and brachiopods (58–61), and (b) the Polyzoa hypothesis, which proposes closer affiliation to Entoprocta and Cycliophora (40, 62, 63) (*SI Appendix*, Fig. S1). Currently, no chromosome-scale genomes are available for Cycliophora, Entoprocta, or Phoronida species, but a chromosome-scale genome of the brachiopod *Lingula anatina* is accessible (PRJNA1068743). We conducted a macrosynteny comparison between the bryozoan *M. membranacea*, representative of Gymnolaemata bryozoans, and the brachiopod *L. anatina* to test for the existence of shared derived rare genomic changes in the form of chromosome fusion-with-mixing events.

We identified nine fusion-with-mixing events shared between *L. anatina* and *M. membranacea* (Fig. 5*A* and *B*). Four of these events (J2⊗L, O1⊗R, O2⊗K, and H⊗Q) are also shared with annelids, nemerteans, and molluscs (Fig. 3) (4, 13). The remaining five fusion-with-mixing events are exclusive to brachiopods and bryozoans, making them shared derived characteristics unique to these groups (Fig. 5*C*). This suggests that bryozoans and brachiopods are closely related, having inherited these changes from a recent common ancestor, supporting the Lophophorata hypothesis (Fig. 5*D,* scenario Type A). The changes could also be attributed to convergent evolution (Type B) or a mixture of inheritance from a common ancestor and convergent evolution (Type C), but inheritance from a recent common ancestor is the most parsimonious explanation, requiring the fewest fusion-with-mixing events (Fig. 5*D*).

Under the assumption that fusion-with-mixing events are irreversible, the Type A scenario would be contradicted if any bryozoan, phoronid, or brachiopod were discovered without the described fusion-with-mixing events. To test this, we examined whether the same

fusion events are present in *Cri. mucedo*, the most divergent bryozoan in our dataset. Despite *Cri. mucedo* having a highly derived chromosome organization, all five derived fusion-with-mixing events shared by *M. membranacea* and *L. anatina* also occur on the same chromosomes in *Cri. mucedo* (*SI Appendix*, Fig. S7). Altogether, we observed nine shared fusion chromosome events between bryozoans and brachiopods, with at least four being derived fusion-with-mixing events and thus considered potential phylogenetic markers. These events are notably absent in molluscs, annelids, and nemerteans, which we interpret as indicating a close relationship between bryozoans and brachiopods, supporting the Lophophorata hypothesis. In the future, sequencing a phoronid genome to chromosome level will be a key test of this hypothesis, revealing whether the same fusions are found in this phylum.

Genome structure and Hox gene evolution.

In bilaterians, Hox genes are essential for body patterning and cell type specification (64), a role facilitated by their organization into tight clusters (65–67). We explored whether extensive genome reshuffling has impacted Hox cluster organization in bryozoans. We annotated the Hox genes of the five bryozoan species (*SI Appendix*, Fig. S8 and Dataset S2) and identified extensive gene loss in the bryozoan Hox gene set, which lacks *Hox1*, *Hox3*, *Scr*, *Antp*, *Lox2*, and *Post1* in all five species. Strikingly, the remaining Hox genes are distributed across two separate chromosomes in every assembly (Fig. 6*A*). In bilaterians such as *P. maximus* and *L. longissimus*, the Hox cluster is associated with the ALG B2. This ALG is fragmented across four chromosomes (five in *Cry. pallasiana*) in each bryozoan genome, as a result of successive fusion and fission events (Fig. 6*B*). The main Hox cluster is located on orthologous chromosomes containing ALG B2 genes in each bryozoan genome assembly, while Hox genes separated from the cluster are also on a different orthologous chromosome that contains ALG B2 genes (Fig. 6*C*). This evidence suggests that the presence of Hox genes across two chromosomes in bryozoans is a unique case of partial cluster tandem duplication (*Hox4*, *Lox5*, *Lox4*, and *Post2* genes) followed by separation due to chromosome fission (Fig. 6*D*).

Given the critical dependence of Hox gene regulation on genomic organization, we hypothesized that physical separation might alter gene expression. To investigate this, we analyzed the expression of bryozoan Hox paralogues located on different chromosomes using existing RNA-sequencing data (*SI Appendix*, Fig. S9 and Table S14). In *Cri. mucedo*, both the *Hox4b* and *Lox5b* genes separated from the main cluster are expressed more highly than their main cluster counterparts, *Hox4a* and *Lox5a* (paired t-tests $p = 0.0009$ and $p = 0.0001$, respectively) (*SI Appendix*, Fig. S9). Therefore, the physical separation of Hox cluster genes by genome rearrangements is associated with differences in expression levels.

Discussion

Our study reveals dramatic rearrangements to bryozoan chromosomes that have largely atomized the 24 conserved bilaterian ALGs. This presents a stark contrast to reports of ALG conservation from other spiralians (12, 13), deuterostomes (6), and even non-bilaterians like cnidarians (4). We propose that a strong evolutionary pressure has held linked genes together since the origin of eumetazoans and that this constraint has been released in the bryozoan lineage. We distinguish two distinct periods of change: the first generating the derived bryozoan ancestral state of just six ALGs from the conserved bilaterian ALGs, and the second modifying this state further in two bryozoan classes.

Genomes exhibiting extensive ALG fusions are uncommon but have been previously documented (4, 14). Nonetheless, three aspects of bryozoan genomes stand out as particularly remarkable. Firstly, the magnitude of chromosome fusions is notable, with 18 out of 24 (75%) bilaterian ALGs on the same chromosomes. Secondly, the widespread occurrence of these massive fusion events across the phylum is exceptionally rare. Unlike dipterans, where such extensive fusion events are specific to certain lineages (4, 68), bryozoans display this phenomenon across the entire phylum. Thirdly, many ALGs in bryozoans have been separated by chromosome fissions. Major studies on animal chromosome evolution suggested that a general rule in metazoans is that ALGs are combined but not broken up (4, 10). In contrast, we identified numerous fissions occurring in the common ancestor of the four Gymnolaemata species around 350 million years ago (51), with subsequent, lineage-specific fission in *Cry. pallasiana* less than 90 million years ago (51). This indicates a prolonged period during which chromosome fissions were evolutionarily tolerated, challenging the notion that fissions occur in brief, time-limited periods and are followed by evolutionary stasis (4).

Why have bryozoans specifically undergone radical ALG fissions while most animal phyla retained the conserved ancestral state? Although our study doesn't offer a definitive answer, we can apply Mayr's classical framework (70) to outline the elements of a possible explanation. Firstly, we must identify the mechanism that generated these rearrangements (the proximate cause). Secondly, we must understand why these rearrangements conferred a fitness advantage and were thus favored by selection (the ultimate cause). The latter, concerning the ultimate cause, is particularly intriguing from an evolutionary standpoint. While previous studies on macrosynteny have extensively explored the selective pressures that favor ALG conservation and retention, such as long-range chromatin interactions and meiotic constraints (4, 10), our focus shifts to why these pressures were overridden in bryozoans. One possibility is that a change in the relative importance of mechanisms of gene regulation placed a reduced emphasis on long-range interactions and rendered conserved genome organization obsolete. Our work highlights the need for studies relating gene regulation to genome organization, which may be key to understanding the ultimate causes of the evolution of highly derived genomic architectures.

Having elucidated the organization of bryozoan genomes, we questioned whether macrosynteny could resolve their phylogenetic position. Substantial evidence has been presented supporting both their association with Phoronida and Brachiopoda (Lophophorata) (58–61) and with Entoprocta and Cycliophora (Polyzoa) (40, 62, 63). Our study identifies nine fusion-with-mixing events shared between bryozoans and brachiopods, of which four are confirmed as derived characters, supporting the Lophophorata topology. Fusion-with-mixing events are essentially irreversible in evolution, but convergent evolution cannot be ruled out (33). If these rare genomic changes are specific to Lophotrochozoans (excluding Entoprocta and Cycliophora), then the presence of at least eight shared derived fusion events in brachiopods and bryozoans would almost rule out convergence, becoming a conclusive piece of evidence in this ongoing debate. The future availability of chromosome-scale genomes from these groups is expected to provide clarity. Looking further, evidence from macrosynteny is likely to become increasingly prominent in discussions concerning phylogenetically challenging clades.

Materials and Methods

Assembly acquisition and gene prediction.

Chromosome-scale assemblies of *B. stolonifera* (GenBank accession no. GCA_935421135) (45), *Cry. pallasiana* (GCA_945261195) (44), *M. membranacea* (GCA_914767715) (43), and

W. subatra (GCA_963576615) were sequenced as part of the Darwin Tree of Life project (48) and retrieved from the NCBI Datasets. A chromosome-scale assembly of *Cri. mucedo (42)* was obtained from the NCBI Gene Expression Omnibus (GSE169088). None of the bryozoan assemblies used have publicly available gene models, so gene prediction was performed in-house. Repetitive elements were first annotated with RepeatModeler (v2.0.4) (71) and masked using RepeatMasker (v4.1.5) in sensitive mode (72). Gene prediction and annotation were performed using the BRAKER3 pipeline (v3.0.3), incorporating hints from RNA sequencing (RNA-seq) data as aligned reads in bam format (73–81). BRAKER3 uses RNA-seq and genome data to train the gene prediction tools AUGUSTUS and GeneMark, producing highly supported gene transcripts. Raw RNA-seq reads for gene prediction (*SI Appendix*, Table S2) were sourced from the NCBI Sequence Read Archive (SRA) using the SRA toolkit (82) with GNU parallel (83). Quality control was performed with FastQC (84). Reads were trimmed with Trimmomatic (v0.39) (85) and aligned to the genome with STAR (v2.7.10b) (86). BUSCO (v5.4.7) (52) was used to evaluate the quality of gene prediction. Hox genes were identified with reciprocal tBLASTn searches (87), and orthology was confirmed using gene trees built in IQ-TREE (v2.2.2.3) (88). Hox annotations are consistent with previous work, where available (89).

Phylogenetics.

Single-copy orthologs were identified using OrthoFinder (v2.5.4) (53). Alignments for each set of orthologs were created with MAFFT (v7.520) (90, 91), trimmed with ClipKIT (v1.4.1) (92), and concatenated with PhyKIT (v1.11.7) (93). IQ-TREE (v2.2.2.3) (88) was used to construct maximum likelihood trees with automated substitution model selection using ModelFinder (94) and 1,000 UFBoot2 ultra-fast bootstrap replicates (95). Trees were rendered with iTOL (96). A tree of Hox protein sequences was generated with the same IQ-TREE method.

Macrosynteny analysis.

OrthoFinder (v2.5.4) (53) was used to identify single-copy orthologs. Two runs were performed: first with only the five bryozoan species, and second adding *B. floridae* (Chordata), *P. maximus* (Mollusca), *L. longissimus* (Nemertea) and *L. anatina* (Brachiopoda). Macrosynteny plots were created with RIdeogram (v0.2.2) (97) in R (v4.3.0) (98). Bilaterian ALGs (4) were used to color synteny plots. In synteny plots, links between chromosomes with fewer than five shared genes were removed for clarity. These represent single-gene or few-gene translocations. Translocated genes are included in Oxford plots. For plotting purposes and to ensure alignment with orthologous chromosomes, the orientations of chromosomes chr1, chr2, chr4, chr6, chr7, chr10, and chr11 in *W. subatra*, and chr2, chr3, chr7, CPA9, chr10, chr11, chr12 in *Cry. pallasiana* were reversed from their orientations as presented in the published datasets.

Quantification of microsynteny mixing score.

To assess the amount of intra-chromosomal gene shuffling, we first calculated Spearman's rank correlation coefficient (ρ). This coefficient quantifies the strength and direction of association between the ranked order of orthologous genes along orthologous chromosome pairs. The Spearman's coefficient is given by the following equation:

$$\rho = 1 - (6 * \Sigma d_i^2) / [n(n^2 - 1)] \quad [1]$$

where ρ is the coefficient, d_i represents the difference in ranks between corresponding values of the two variables, and n is the total number of observations. Subsequently, we defined the synteny mixing score, an indicator of chromosomal rearrangement, using the equation:

$$1 - |\rho| \qquad [2]$$

where $|\rho|$ denotes the absolute value of the Spearman's coefficient. This metric allows the synteny mixing score to vary from 0, indicative of no intra-chromosomal rearrangement and thus a high degree of conserved microsynteny, to 1, representative of maximum rearrangement, signifying considerable disruption in the original gene order.

Estimation of species divergence time.
A phylogenetic tree, constructed above from single-copy orthologs extracted from five bryozoan genomes and a mollusc outgroup (*P. maximus*), was used to estimate divergence times. We calibrated this tree with contemporary molecular and fossil data (51), focusing on the divergence between *P. maximus* and *Cri. mucedo* during the Cambrian Period (541 to 488 million years ago) (47), employing the ape package in R (99).

Quantification of gene expression.
Gene expression was quantified in published *B. stolonifera* (PRJNA607082) and *Cri. mucedo* (PRJNA594616) RNA-seq datasets. Raw reads were obtained from the NCBI SRA using the SRA toolkit (82) and GNU parallel (83). Hox gene expression was quantified with Salmon (v1.10.2) (100). *Hox4a*, *Hox4b*, *Lox5a*, and *Lox5b* gene expression levels were compared using *t*-tests with a Benjamini-Hochberg correction for multiple testing.

Data availability.
Gene models for all five bryozoan species have been deposited in Dryad (https://doi.org/10.5061/dryad.76hdr7t3f). Custom Python and R scripts used for macrosynteny analysis, calculating mixing scores, and estimating divergence times are available in our GitHub repository (https://github.com/symgenoevolab/SyntenyFinder).

Acknowledgments
This work was funded by a Royal Society Newton International Fellowship (NIF\R1\201315) and an Academia Sinica Career Development Award (AS-CDA-112-L06) to Y.-J.L. We acknowledge the efforts in sample collection by the Marine Biological Association (MBA)–Darwin Tree of Life collecting team: Patrick Adkins, Robert Mrowicki, Joanna Harley, and Helen Jenkins, as well as Christine Wood of the MBA. We thank the members of the Symbiosis Genomics & Evolution Lab for their assistance and support.

Author contributions:
T.D.L. and Y.-J.L. designed research; T.D.L., I.J.-Y.L., M.-E.C., and Y.-J.L. performed research; T.D.L., I.J.-Y.L., J.D.D.B., and Y.-J.L. contributed new reagents/analytic tools; T.D.L. and Y.-J.L. analyzed data; and T.D.L., P.W.H.H., and Y.-J.L. wrote the paper.

Competing interests: The authors declare no competing interest.

References

1. N. H. Putnam, *et al.*, Sea anemone genome reveals ancestral eumetazoan gene repertoire and genomic organization. *Science* **317**, 86–94 (2007).
2. N. H. Putnam, *et al.*, The amphioxus genome and the evolution of the chordate karyotype. *Nature* **453**, 1064–1071 (2008).
3. O. Simakov, *et al.*, Insights into bilaterian evolution from three spiralian genomes. *Nature* **493**, 526–531 (2013).
4. O. Simakov, *et al.*, Deeply conserved synteny and the evolution of metazoan chromosomes. *Sci. Adv.* **8**, eabi5884 (2022).
5. D. T. Schultz, *et al.*, Ancient gene linkages support ctenophores as sister to other animals. *Nature* **618**, 110–117 (2023).
6. C.-Y. Lin, *et al.*, Chromosome-level genome assemblies of two hemichordates provide new insights into deuterostome origin and chromosome evolution. *bioRxiv*, 2023.11.01.564642 (2023).
7. A. Mackintosh, P. M. G. de la Rosa, S. H. Martin, K. Lohse, D. R. Laetsch, Inferring inter-chromosomal rearrangements and ancestral linkage groups from synteny. *bioRxiv*, 2023.09.17.558111 (2023).
8. C. Sacerdot, A. Louis, C. Bon, C. Berthelot, H. Roest Crollius, Chromosome evolution at the origin of the ancestral vertebrate genome. *Genome Biol.* **19**, 166 (2018).
9. O. Simakov, *et al.*, Deeply conserved synteny resolves early events in vertebrate evolution. *Nat. Ecol. Evol.* **4**, 820–830 (2020).
10. C. J. Wright, L. Stevens, A. Mackintosh, M. Lawniczak, M. Blaxter, Chromosome evolution in Lepidoptera. *bioRxiv*, 2023.05.12.540473 (2023).
11. F. Marlétaz, *et al.*, Analysis of the P. lividus sea urchin genome highlights contrasting trends of genomic and regulatory evolution in deuterostomes. *Cell Genom.* **3**, 100295 (2023).
12. S. Wang, *et al.*, Scallop genome provides insights into evolution of bilaterian karyotype and development. *Nat. Ecol. Evol.* **1**, 120 (2017).
13. F. M. Martín-Zamora, *et al.*, Annelid functional genomics reveal the origins of bilaterian life cycles. *Nature* **615**, 105–110 (2023).
14. M. Ivankovic, *et al.*, A comparative analysis of planarian genomes reveals regulatory conservation in the face of rapid structural divergence. *bioRxiv*, 2023.12.22.572568 (2023).
15. C. Plessy, *et al.*, Extreme genome scrambling in cryptic Oikopleura dioica species. *bioRxiv*, 2023.05.09.539028 (2023).
16. C. Román-Palacios, C. A. Medina, S. H. Zhan, M. S. Barker, Animal chromosome counts reveal a similar range of chromosome numbers but with less polyploidy in animals compared to flowering plants. *J. Evol. Biol.* **34**, 1333–1339 (2021).
17. A. Rice, *et al.*, The Chromosome Counts Database (CCDB) - a community resource of plant chromosome numbers. *New Phytol.* **206**, 19–26 (2015).
18. M. J. D. White, *Animal cytology & evolution* (Cambridge university press, 1954).
19. M. King, *Species Evolution: The Role of Chromosome Change* (Cambridge University Press, 1995).
20. H. A. Orr, “Why Polyploidy is Rarer in Animals Than in Plants” Revisited. *Am. Nat.* **136**, 759–770 (1990).
21. T. R. Gregory, B. K. Mable, “CHAPTER 8 - Polyploidy in Animals” in *The Evolution of the Genome*, T. R. Gregory, Ed. (Academic Press, 2005), pp. 427–517.

22. Y. Moriyama, K. Koshiba-Takeuchi, Significance of whole-genome duplications on the emergence of evolutionary novelties. *Brief. Funct. Genomics* **17**, 329–338 (2018).
23. M. Muffato, *et al.*, Reconstruction of hundreds of reference ancestral genomes across the eukaryotic kingdom. *Nat. Ecol. Evol.* **7**, 355–366 (2023).
24. L. Harewood, P. Fraser, The impact of chromosomal rearrangements on regulation of gene expression. *Hum. Mol. Genet.* **23**, R76–82 (2014).
25. K. Yoshida, *et al.*, Chromosome fusions repatterned recombination rate and facilitated reproductive isolation during Pristionchus nematode speciation. *Nat. Ecol. Evol.* **7**, 424–439 (2023).
26. S. Coyle, E. Kroll, Starvation Induces Genomic Rearrangements and Starvation-Resilient Phenotypes in Yeast. *Mol. Biol. Evol.* **25**, 310–318 (2007).
27. M. J. Dunham, *et al.*, Characteristic genome rearrangements in experimental evolution of Saccharomyces cerevisiae. *Proc. Natl. Acad. Sci. U.S.A.* **99**, 16144–16149 (2002).
28. C. Cheng, *et al.*, Ecological genomics of Anopheles gambiae along a latitudinal cline: a population-resequencing approach. *Genetics* **190**, 1417–1432 (2012).
29. L. H. Rieseberg, Chromosomal rearrangements and speciation. *Trends Ecol. Evol.* **16**, 351–358 (2001).
30. J. M. de Vos, H. Augustijnen, L. Bätscher, K. Lucek, Speciation through chromosomal fusion and fission in Lepidoptera. *Philos. Trans. R. Soc. Lond. B Biol. Sci.* **375**, 20190539 (2020).
31. E. L. Berdan, *et al.*, Structural Variants and Speciation: Multiple Processes at Play. *Cold Spring Harb. Perspect. Biol.* a041446 (2023).
32. A. Mackintosh, *et al.*, Chromosome fissions and fusions act as barriers to gene flow between Brenthis fritillary butterflies. *Mol. Biol. Evol.* **40** (2023).
33. J. Steenwyk, N. King, From genes to genomes: Opportunities, challenges, and a roadmap for synteny-based phylogenomics. *Preprints* (2024) https:/doi.org/10.20944/preprints202309.0495.v2.
34. E. Parey, *et al.*, Genome structures resolve the early diversification of teleost fishes. *Science* **379**, 572–575 (2023).
35. R. A. Jenner, D. T. J. Littlewood, Problematica old and new. *Philos. Trans. R. Soc. Lond. B Biol. Sci.* **363**, 1503–1512 (2008).
36. R. A. Jenner, D. Timothy, J. Littlewood, 'Invertebrate Problematica: kinds, causes, and solutions' in Maximilian J. Telford, and D.T.J. Littlewood (eds), Animal Evolution: Genomes, Fossils, and Trees (Oxford, 2009).
37. J. Loxton, *et al.*, Distribution of the invasive bryozoan Schizoporella japonica in Great Britain and Ireland and a review of its European distribution. *Biol. Invasions* **19**, 2225–2235 (2017).
38. H. Weaver, P. Cook, P. Bock, D. Gordon, *Australian Bryozoa Volume 1: Biology, Ecology and Natural History* (Csiro Publishing, 2018).
39. C. Pratt, D. Denley, A. Metaxas, Ocean warming and multiple source populations increase the threat of an invasive bryozoan to kelp beds in the northwest Atlantic Ocean. *Mar. Ecol. Prog. Ser.* **695**, 65–81 (2022).
40. K. Khalturin, *et al.*, Polyzoa is back: The effect of complete gene sets on the placement of Ectoprocta and Entoprocta. *Sci Adv* **8**, eabo4400 (2022).
41. Z. Zhang, *et al.*, Fossil evidence unveils an early Cambrian origin for Bryozoa. *Nature* **599**, 251–255 (2021).
42. C. Hoencamp, *et al.*, 3D genomics across the tree of life reveals condensin II as a determinant of architecture type. *Science* **372**, 984–989 (2021).

43. J. Bishop, *et al.*, The genome sequence of the sea mat, Membranipora membranacea (Linnaeus, 1767). *Wellcome Open Res.* **8**, 38 (2023).
44. J. Bishop, *et al.*, The genome sequence of an encrusting bryozoan, Cryptosula pallasiana (Moll, 1803). *Wellcome Open Res.* **8**, 128 (2023).
45. C. Wood, *et al.*, The genome sequence of an erect bryozoan, Bugulina stolonifera (Ryland, 1960). *Wellcome Open Res.* **8**, 26 (2023).
46. I. J.-Y. Liao, T.-M. Lu, M.-E. Chen, Y.-J. Luo, Spiralian genomics and the evolution of animal genome architecture. *Brief. Funct. Genomics* **6**, 498–508 (2023).
47. D. H. Erwin, *et al.*, The Cambrian conundrum: early divergence and later ecological success in the early history of animals. *Science* **334**, 1091–1097 (2011).
48. T. D. T. of Life Project Consortium, *et al.*, Sequence locally, think globally: The Darwin Tree of Life Project. *Proc. Natl. Acad. Sci. U.S.A.* **119**, e2115642118 (2022).
49. P. E. Bock, D. P. Gordon, [No title]. *Zootaxa* **3703**, 67–74 (2013).
50. P. D. Taylor, A. Waeschenbach, Phylogeny and diversification of bryozoans. *Palaeontology* **58**, 585–599 (2015).
51. R. J. S. Orr, *et al.*, Paleozoic origins of cheilostome bryozoans and their parental care inferred by a new genome-skimmed phylogeny. *Sci. Adv.* **8**, eabm7452 (2022).
52. F. A. Simão, R. M. Waterhouse, P. Ioannidis, E. V. Kriventseva, E. M. Zdobnov, BUSCO: assessing genome assembly and annotation completeness with single-copy orthologs. *Bioinformatics* **31**, 3210–3212 (2015).
53. D. M. Emms, S. Kelly, OrthoFinder: phylogenetic orthology inference for comparative genomics. *Genome Biol.* **20**, 238 (2019).
54. J. H. Renwick, THE MAPPING OF HUMAN CHROMOSOMES. *Annu. Rev. Genet.* **5**, 81–120 (1971).
55. E. Passarge, B. Horsthemke, R. A. Farber, Incorrect use of the term synteny. *Nat. Genet.* **23**, 387 (1999).
56. D. Kwiatkowski, *et al.*, The genome sequence of the bootlace worm, Lineus longissimus (Gunnerus, 1770). *Wellcome Open Res.* **6**, 272 (2021).
57. N. J. Kenny, *et al.*, The gene-rich genome of the scallop Pecten maximus. *Gigascience* **9** (2020).
58. M. P. Nesnidal, *et al.*, New phylogenomic data support the monophyly of Lophophorata and an Ectoproct-Phoronid clade and indicate that Polyzoa and Kryptrochozoa are caused by systematic bias. *BMC Evol. Biol.* **13**, 253 (2013).
59. Y.-J. Luo, *et al.*, Nemertean and phoronid genomes reveal lophotrochozoan evolution and the origin of bilaterian heads. *Nat. Ecol. Evol.* **2**, 141–151 (2017).
60. F. Marlétaz, K. T. C. A. Peijnenburg, T. Goto, N. Satoh, D. S. Rokhsar, A New Spiralian Phylogeny Places the Enigmatic Arrow Worms among Gnathiferans. *Curr. Biol.* **29**, 312–318.e3 (2019).
61. C. E. Laumer, *et al.*, Revisiting metazoan phylogeny with genomic sampling of all phyla. *Proc. R. Soc. B* **286**, 20190831 (2019).
62. A. Hejnol, *et al.*, Assessing the root of bilaterian animals with scalable phylogenomic methods. *Proc. R. Soc. B* **276**, 4261–4270 (2009).
63. K. M. Kocot, *et al.*, Phylogenomics of Lophotrochozoa with Consideration of Systematic Error. *Syst. Biol.* **66**, 256–282 (2017).
64. K. A. Hubert, D. M. Wellik, Hox genes in development and beyond. *Development* **150** (2023).
65. M. Akam, Hox and HOM: homologous gene clusters in insects and vertebrates. *Cell* **57**, 347–349 (1989).

66. A. Graham, N. Papalopulu, R. Krumlauf, The murine and Drosophila homeobox gene complexes have common features of organization and expression. *Cell* **57**, 367–378 (1989).
67. D. Duboule, P. Dollé, The structural and functional organization of the murine HOX gene family resembles that of Drosophila homeotic genes. *EMBO J.* **8**, 1497–1505 (1989).
68. E. M. Zdobnov, C. von Mering, I. Letunic, P. Bork, Consistency of genome-based methods in measuring Metazoan evolution. *FEBS Lett.* **579**, 3355–3361 (2005).
69. A. D. Chipman, *et al.*, The first myriapod genome sequence reveals conservative arthropod gene content and genome organisation in the centipede *Strigamia maritima*. *PLoS Biol.* **12**, e1002005 (2014).
70. E. Mayr, Cause and Effect in Biology. *Science* **134**, 1501–1506 (1961).
71. J. M. Flynn, *et al.*, RepeatModeler2 for automated genomic discovery of transposable element families. *Proc. Natl. Acad. Sci. U.S.A.* **117**, 9451–9457 (2020).
72. A. F. A. Smit, R. Hubley, P. Green, RepeatMasker Open-4.0 (2015).
73. M. Stanke, O. Schöffmann, B. Morgenstern, S. Waack, Gene prediction in eukaryotes with a generalized hidden Markov model that uses hints from external sources. *BMC Bioinformatics* **7**, 62 (2006).
74. M. Stanke, M. Diekhans, R. Baertsch, D. Haussler, Using native and syntenically mapped cDNA alignments to improve de novo gene finding. *Bioinformatics* **24**, 637–644 (2008).
75. H. Li, *et al.*, The Sequence Alignment/Map format and SAMtools. *Bioinformatics* **25**, 2078–2079 (2009).
76. D. W. Barnett, E. K. Garrison, A. R. Quinlan, M. P. Strömberg, G. T. Marth, BamTools: a C++ API and toolkit for analyzing and managing BAM files. *Bioinformatics* **27**, 1691–1692 (2011).
77. A. Lomsadze, P. D. Burns, M. Borodovsky, Integration of mapped RNA-Seq reads into automatic training of eukaryotic gene finding algorithm. *Nucleic Acids Res.* **42**, e119 (2014).
78. B. Buchfink, C. Xie, D. H. Huson, Fast and sensitive protein alignment using DIAMOND. *Nat. Methods* **12**, 59–60 (2015).
79. K. J. Hoff, S. Lange, A. Lomsadze, M. Borodovsky, M. Stanke, BRAKER1: Unsupervised RNA-Seq-Based Genome Annotation with GeneMark-ET and AUGUSTUS. *Bioinformatics* **32**, 767–769 (2016).
80. K. J. Hoff, A. Lomsadze, M. Borodovsky, M. Stanke, Whole-Genome Annotation with BRAKER. *Methods Mol. Biol.* **1962**, 65–95 (2019).
81. T. Brůna, K. J. Hoff, A. Lomsadze, M. Stanke, M. Borodovsky, BRAKER2: automatic eukaryotic genome annotation with GeneMark-EP+ and AUGUSTUS supported by a protein database. *NAR Genom. Bioinform.* **3**, lqaa108 (2021).
82. R. Leinonen, H. Sugawara, M. Shumway, International Nucleotide Sequence Database Collaboration, The sequence read archive. *Nucleic Acids Res.* **39**, D19–21 (2011).
83. O. Tange, *GNU Parallel 2018* (Lulu.com, 2018).
84. S. Andrews, Others, FastQC: a quality control tool for high throughput sequence data (2010).
85. A. M. Bolger, M. Lohse, B. Usadel, Trimmomatic: a flexible trimmer for Illumina sequence data. *Bioinformatics* **30**, 2114–2120 (2014).
86. A. Dobin, *et al.*, STAR: ultrafast universal RNA-seq aligner. *Bioinformatics* **29**, 15–21 (2013).
87. C. Camacho, *et al.*, BLAST+: architecture and applications. *BMC Bioinformatics* **10**, 421

(2009).
88. B. Q. Minh, *et al.*, IQ-TREE 2: New Models and Efficient Methods for Phylogenetic Inference in the Genomic Era. *Mol. Biol. Evol.* **37**, 1530–1534 (2020).
89. A. J. Saadi, A. L. de Oliveira, K. M. Kocot, T. Schwaha, Genomic and transcriptomic survey of bryozoan Hox and ParaHox genes with emphasis on phylactolaemate bryozoans. *BMC Genomics* **24**, 711 (2023).
90. K. Katoh, K. Misawa, K.-I. Kuma, T. Miyata, MAFFT: a novel method for rapid multiple sequence alignment based on fast Fourier transform. *Nucleic Acids Res.* **30**, 3059–3066 (2002).
91. K. Katoh, D. M. Standley, MAFFT multiple sequence alignment software version 7: improvements in performance and usability. *Mol. Biol. Evol.* **30**, 772–780 (2013).
92. J. L. Steenwyk, T. J. Buida 3rd, Y. Li, X.-X. Shen, A. Rokas, ClipKIT: A multiple sequence alignment trimming software for accurate phylogenomic inference. *PLoS Biol.* **18**, e3001007 (2020).
93. J. L. Steenwyk, *et al.*, PhyKIT: a broadly applicable UNIX shell toolkit for processing and analyzing phylogenomic data. *Bioinformatics* **37**, 2325–2331 (2021).
94. S. Kalyaanamoorthy, B. Q. Minh, T. K. F. Wong, A. von Haeseler, L. S. Jermiin, ModelFinder: fast model selection for accurate phylogenetic estimates. *Nat. Methods* **14**, 587–589 (2017).
95. D. T. Hoang, O. Chernomor, A. von Haeseler, B. Q. Minh, L. S. Vinh, UFBoot2: Improving the Ultrafast Bootstrap Approximation. *Mol. Biol. Evol.* **35**, 518–522 (2018).
96. I. Letunic, P. Bork, Interactive Tree Of Life (iTOL) v5: an online tool for phylogenetic tree display and annotation. *Nucleic Acids Res.* **49**, W293–W296 (2021).
97. Z. Hao, *et al.*, RIdeogram: drawing SVG graphics to visualize and map genome-wide data on the idiograms. *PeerJ Comput. Sci.* **6**, e251 (2020).
98. R. Core Team, R: A language and environment for statistical computing. Vienna: R foundation for statistical computing (2021).
99. E. Paradis, K. Schliep, ape 5.0: an environment for modern phylogenetics and evolutionary analyses in R. *Bioinformatics* **35**, 526–528 (2018).
100. R. Patro, G. Duggal, M. I. Love, R. A. Irizarry, C. Kingsford, Salmon provides fast and bias-aware quantification of transcript expression. *Nat. Methods* **14**, 417–419 (2017).

Figures

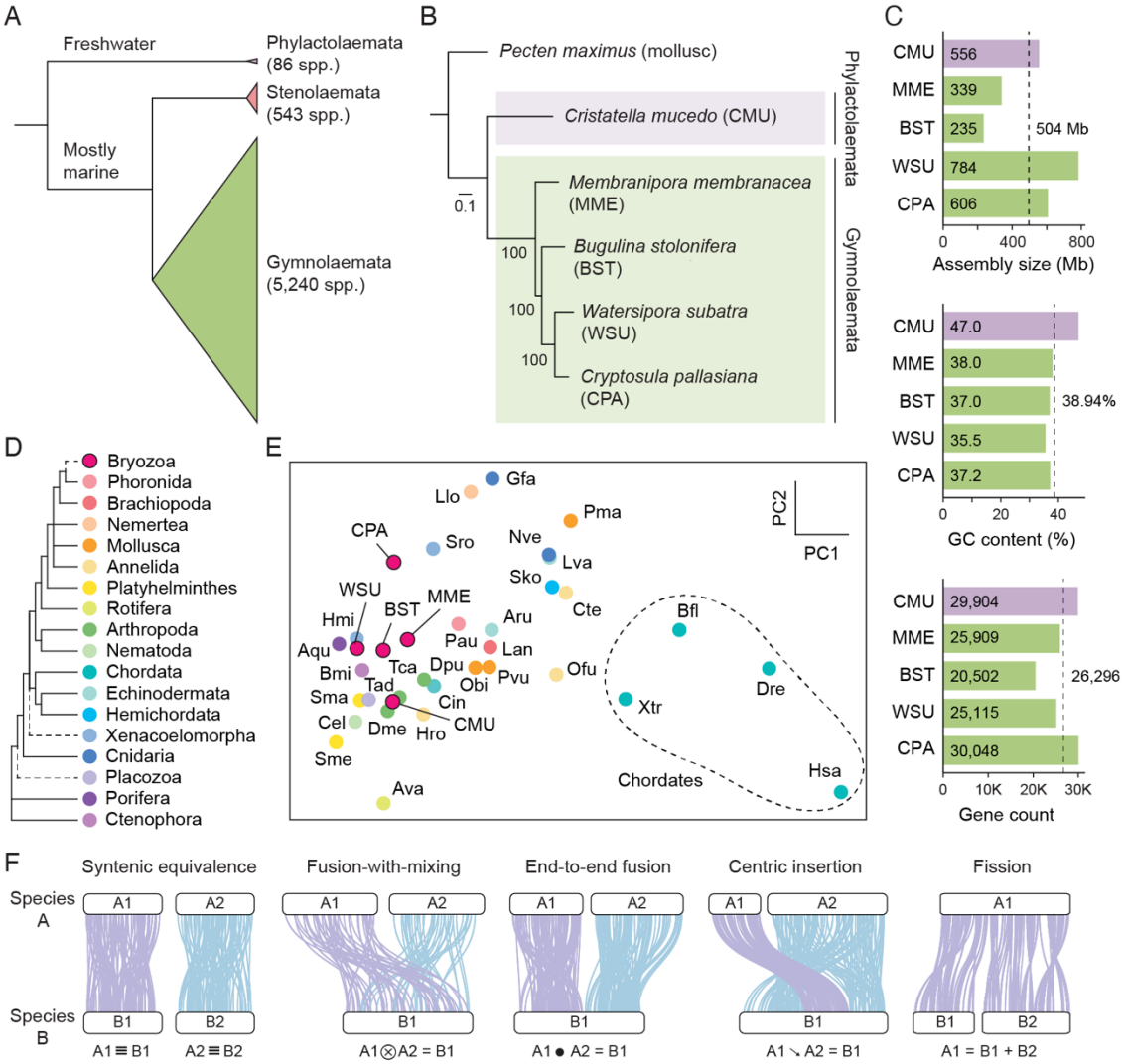

Fig. 1. Comparative genomics of five chromosome-scale bryozoan genomes and schematics of potential chromosome rearrangements. (*A*) Relationships between the three classes of bryozoans. Class Phylactolaemata is the most basal, containing just 86 species, all of which inhabit a freshwater environment (49). Stenolaemata comprises 543 species, all of which are exclusively marine. Gymnolaemata is the most species-rich class, comprising 5,240 species. (*B*) Tree of bryozoan species constructed with chromosome-scale genomes. The tree was constructed using the maximum likelihood method (LG+F+R6 model) with 1,000 bootstrap replicates in IQ-TREE, utilizing 994 orthologous genes. The scallop *Pecten maximus* is the outgroup. (*C*) Genome size, GC content, and gene model count of bryozoan genome assemblies used in this work. Dashed lines mark mean values. The clade containing *W. subatra* and *Cry. pallasiana* has undergone a genome size expansion. (*D*) Phylogenetic relationships among animal phyla, with dashed lines indicating areas of uncertainty in their placement. (*E*) Principal component (PC) analysis conducted using orthologous gene group counts as determined by OrthoFinder. Points are colored by their phylum. (*F*) Schematic representations of possible inter-chromosomal rearrangements. White bars represent chromosomes; colored lines connect orthologous genes; the same color line represents genes in the same ancestral linkage group. Species abbreviations: Ava, *Adineta vaga*; Aqu,

Amphimedon queenslandica; Aru, *Asterias rubens*; Bfl, *Branchiostoma floridae*; Bmi, *Bolinopsis microptera*; Cel, *Caenorhabditis elegans*; Cin, *Ciona intestinalis*; Cte, *Capitella teleta*; Dme, *Drosophila melanogaster*; Dpu, *Daphnia pulex*; Dre, *Danio rerio*; Gfa, *Galaxea fascicularis*; Hmi, *Hofstenia miamia*; Hro, *Helobdella robusta*; Hsa, *Homo sapiens*, Lan, *Lingula anatina*; Llo, *Lineus longissimus*; Lva, *Lytechinus variegatus*; Nve, *Nematostella vectensis*; Obi, *Octopus bimaculoides*; Ofu, *Owenia fusiformis*; Pau, *Phoronis australis*; Pma, *Pecten maximus*; Pvu, *Patella vulgata*; Sko, *Saccoglossus kowalevskii*; Sma, *Schistosoma mansoni*; Sme, *Schmidtea mediterranea*; Sro, *Symsagittifera roscoffensis*; Tad, *Trichoplax adhaerens*; Tca, *Tribolium castaneum*; Xtr, *Xenopus tropicalis*.

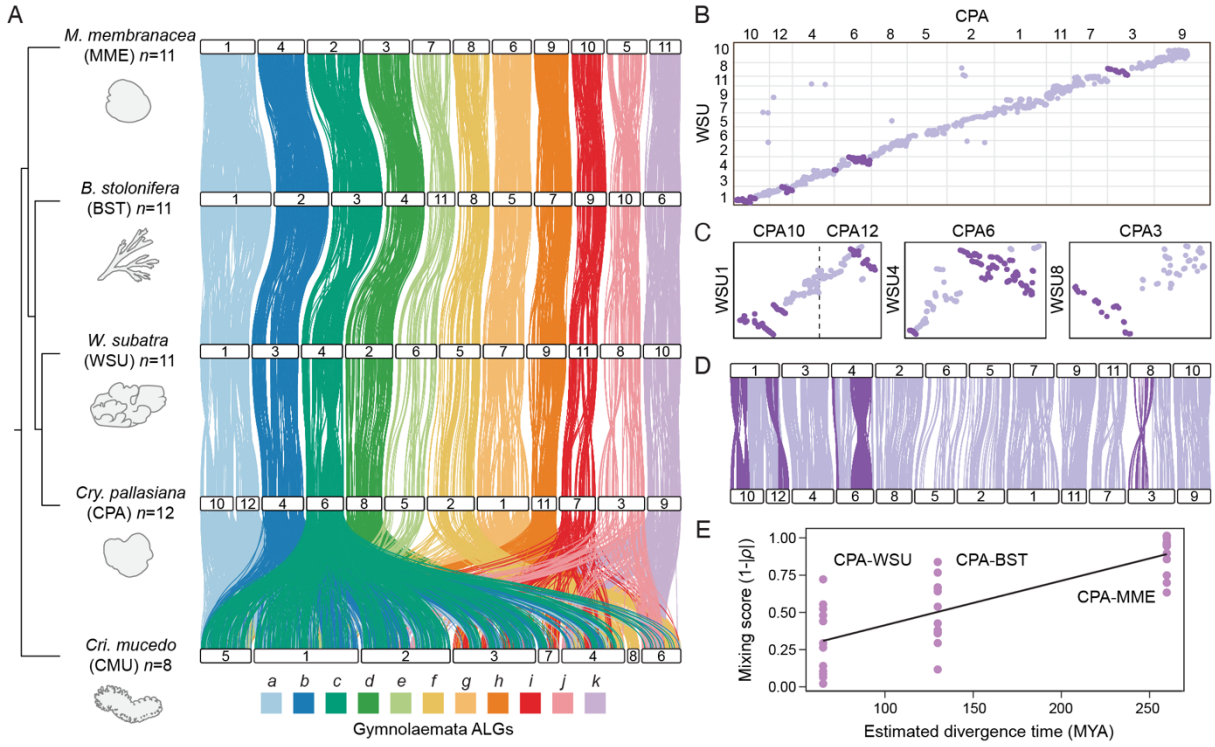

Fig. 2. Chromosome rearrangement in Gymnolaemata and Phylactolaemata bryozoans. (*A*) Chromosome-scale gene linkage between five bryozoan species revealed by ribbon plots. Horizontal bars represent chromosomes. Vertical lines connect the genomic position of orthologous genes in each genome. Chromosomes connected by many orthologs are inferred to be homologous (i.e., orthologous chromosomes). In Gymnolaemata species, 11 ALGs *a* to *k* are highly conserved, though the chromosome containing ALG *a* underwent a fission event to form chromosomes CPA10 and CPA12 in *Cry. pallasiana*. These ALGs are not conserved in the Phylactolaemata species *Cri. mucedo*. Links between chromosomes sharing five or fewer genes between chromosomes are removed for clarity but can be seen in Oxford dot plots (*SI Appendix*, Fig. S1). (*B*) Oxford dot plot revealing chromosome-scale gene linkage between the two most closely related species in our dataset, *Cry. pallasiana* and *W. subatra*. Each axis represents the entire length of the genome of one species. Grey bars separate chromosomes. Each point represents a pair of orthologs placed by their ordinal position in each genome. Strings of orthologs perpendicular to the main bottom-left to the top-right axis reveal clear intra-chromosomal inversions (dark purple). (*C*) Single-chromosome Oxford dot plots for *Cry. pallasiana* and *W. subatra* chromosomes with clear inversions (dark purple). (*D*) Ribbon plot for *Cry. pallasiana* and *W. subatra* highlighting intra-chromosomal inversions (dark purple) (*E*) Microsynteny mixing score versus divergence time for bryozoan chromosomes. Each point represents a chromosome. Microsynteny mixing score measures how genes are shuffled within a chromosome by intra-chromosomal inversions (see Materials and Methods): a higher score indicates more mixing. Mixing score increases with phylogenetic distance. Abbreviation: MYA, million years ago.

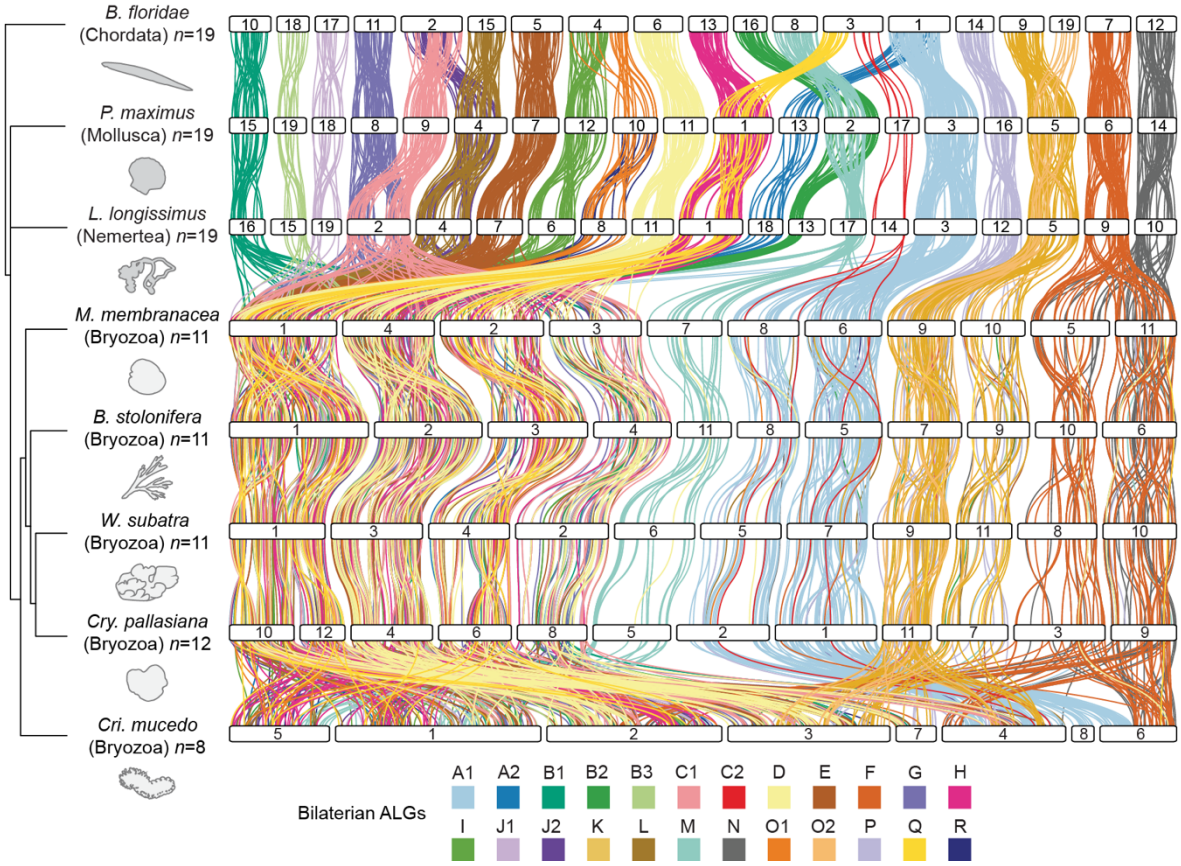

Fig. 3. Extensive fusion-with-mixing of bilaterian ancestral linkage groups in bryozoans. Chromosome-scale gene linkage between five bryozoan species and three outgroup bilaterians: a nemertean, a mollusc, and a chordate. Horizontal bars represent chromosomes. Vertical lines connect the genomic position of orthologous genes in each genome. Lines are colored by the bilaterian ALGs defined by (4). These bilaterian ALGs are highly conserved from the amphioxus *Branchiostoma floridae* to the scallop *Pecten maximus* to the nemertean *Lineus longissimus*, but are highly shuffled in bryozoans.

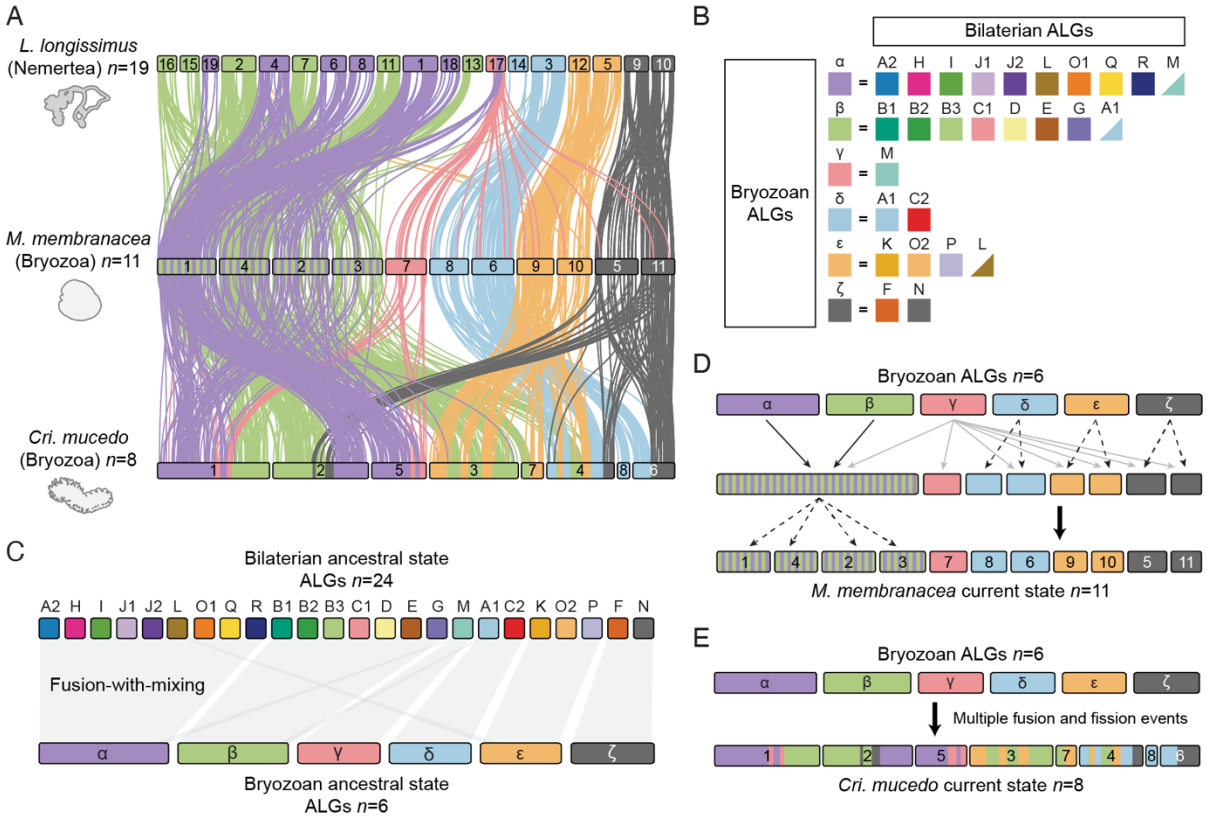

Fig. 4. Reconstruction of bryozoan ancestral genome architecture. (*A*) Chromosome-scale gene linkage between *L. longissimus*, *M. membranacea,* and *Cri. mucedo*. Links between orthologs are colored by their 6 bryozoan ALGs. (*B*) Composition of bryozoan ALGs by bilaterian ALGs, alongside the reconstructed bryozoan ancestral state (6 chromosomes: α, β, γ, δ, ε, and ζ). Triangles indicate the inclusion of several genes from the bilaterian ALG but the majority of genes from that ALG are elsewhere. (*C*) Reconstruction of the genome rearrangements that formed the bryozoan ancestral state. The top row shows bilaterian ALGs, and the bottom row shows bryozoan ALGs. (*D*) Reconstruction of the genome rearrangements that led from the bryozoan ancestral state to the extant Gymnolaemata genomes. Solid black arrows indicate fusion-with-mixing. Solid gray arrows indicate dispersal around the genome. Dashed arrows indicate chromosome fission. (*E*) Reconstruction of the genome rearrangements that led from the bryozoan ancestral state to the extant Phylactolaemata genomes.

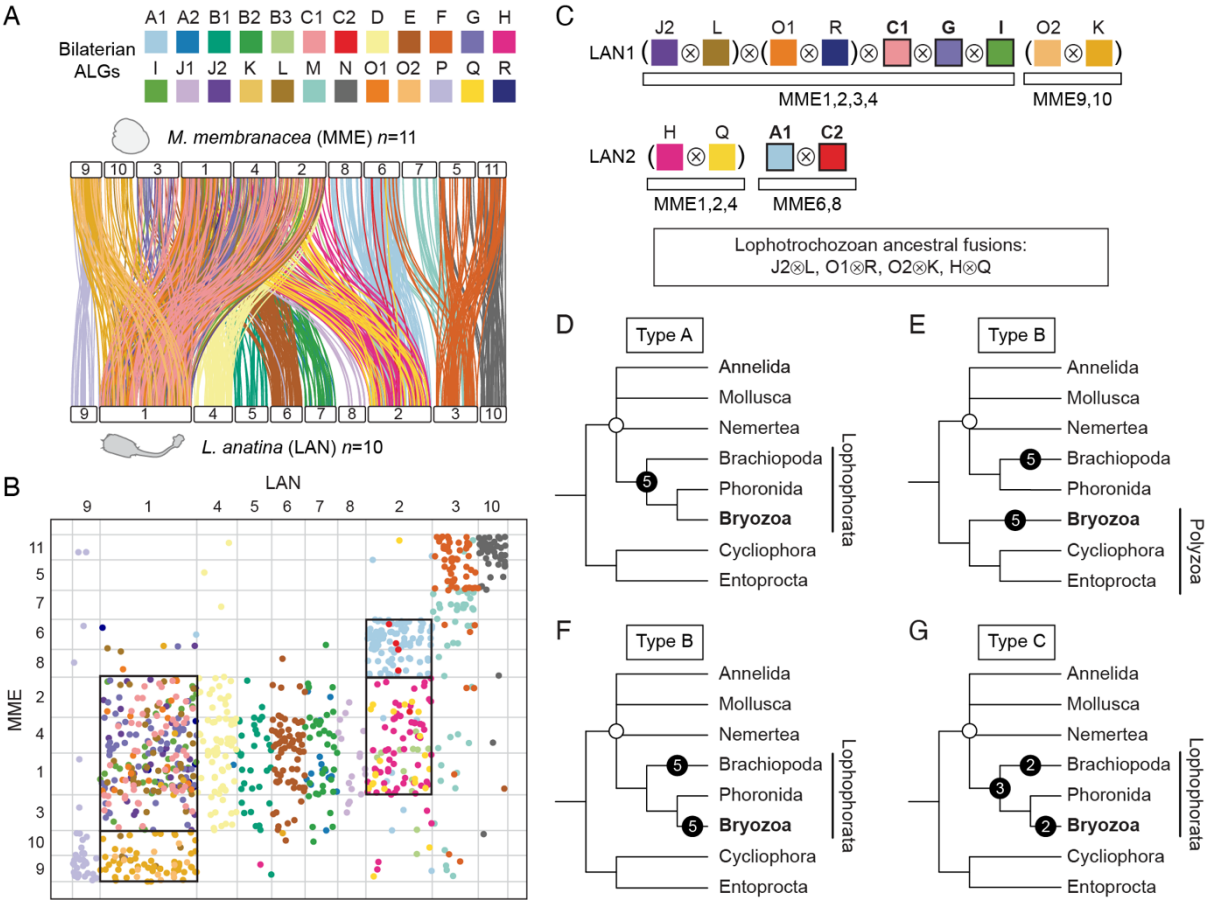

Fig. 5. Shared derived chromosome features between bryozoans and brachiopods support the Lophophorata hypothesis. (*A*) Chromosome-scale gene linkage between the bryozoan *M. membranacea* and the brachiopod *L. anatina*. Horizontal bars represent chromosomes. Vertical lines connect the genomic position of orthologous genes in each genome. Lines are colored by bilaterian ALGs. (*B*) Oxford dot plot revealing chromosome-scale gene linkage between *L. anatina* and *M. membranacea*. Each point represents a pair of orthologs placed by their ordinal position in each genome. Black boxes highlight shared fusion-with-mixing events. (*C*) There are nine shared fusion-with-mixing events between *L. anatina* and *M. membranacea*. Several spiralian phyla share four events ('lophotrochozoan ancestral fusions'), but their timing is uncertain. These events may, therefore, not be useful phylogenetic markers for the position of bryozoans. The remaining five events are derived from fusions shared by bryozoans and brachiopods. (*D*–*G*) Visual representation of four possible evolutionary scenarios that could give rise to the five fusion-with-mixing events shared between bryozoans and brachiopods (Types A, B, and C). An open circle marks the base of the Lophotrochozoa. Black circles mark chromosome fusion-with-mixing events. (*D*) Scenario Type A: Brachiopods, phoronids, and bryozoans are closely related, forming the Lophophorata. The five fusion-with-mixing events shared between bryozoans and *L. anatina* occurred in the ancestor of the Lophophorata. Total number of fusions required: 5. (*E*) Scenario Type B-1: Bryozoans, Cycliophora, and Entoprocta are closely related, forming the Polyzoa. Bryozoans are distantly related to brachiopods. The five fusion-with-mixing events shared between bryozoans and *L. anatina* occurred independently in bryozoans and brachiopods. Total number of fusions required: 10. (*F*) Scenario Type B-2: Brachiopods, phoronids, and bryozoans are closely related, forming the Lophophorata. The five fusion-with-

mixing events shared between bryozoans and *L. anatina* occurred independently in bryozoans and brachiopods. Total number of fusions required: 10. (*G*) Scenario Type C: Brachiopods, phoronids, and bryozoans are closely related, forming the Lophophorata. Some of the five fusion-with-mixing events shared between bryozoans and *L. anatina* occurred in the ancestor of Lophophorata, while some occurred independently in bryozoans and brachiopods. Total number of fusions required: 6–9.

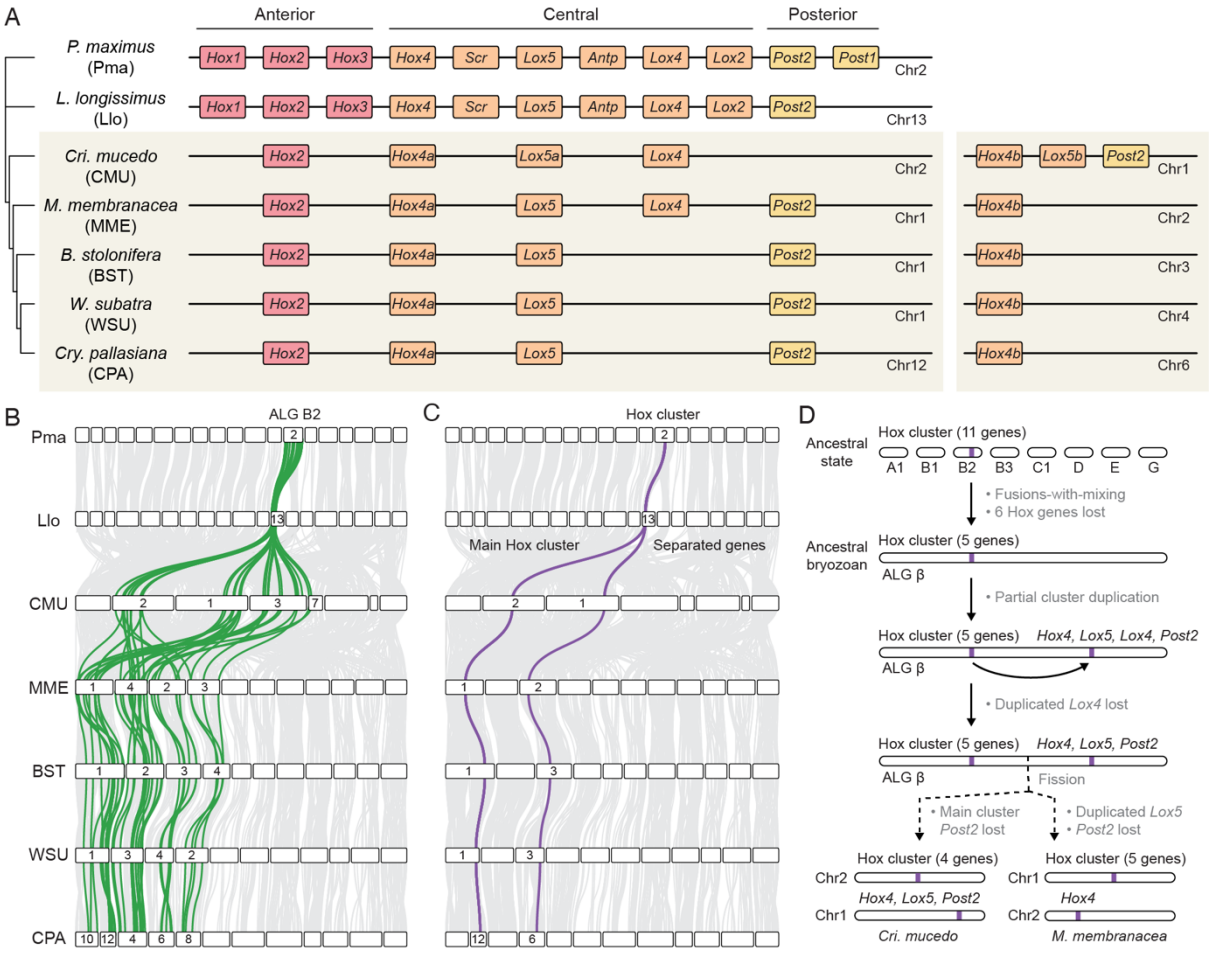

Fig. 6. Evolution of the bryozoan Hox cluster. (*A*) Left: Representation of the main Hox cluster of bryozoans and two outgroups, the nemertean *L. longissimus* and the mollusc *P. maximus*. Colored rectangles represent Hox genes. Horizontal black lines represent chromosomes. Right: Separate Hox genes located in different chromosomes. (*B*) Positions of ALG B2 genes (green) in bryozoan genomes. (*C*) Positions of Hox genes (purple) in bryozoan genomes. (*D*) Representation of the evolutionary events that resulted in observed bryozoan Hox gene arrangements. In the bryozoan ancestral lineage, chromosomes containing bilaterian ALGs A1, B1, B2 (including the Hox cluster), B3, C1, D, E, and G underwent sequential fusion events to form bryozoan ALG β; the Hox cluster underwent a partial duplication, copying genes *Hox4*, *Lox5*, *Lox4*, and *Post2*; and the duplicated *Lox4* gene was subsequently lost. In the lineage leading to *Cri. mucedo* (Phylactolaemata), the main cluster *Post2* was lost, and the chromosome containing ALG β underwent fission, leaving the main cluster on chr2 and duplicated genes on chr1. In the lineage leading to *M. membranacea* (Gymnolaemata), the duplicated *Lox5* and *Post2* were lost, and the chromosome containing ALG β underwent fission, leaving the main cluster on chr1 and duplicated genes on chr2.